Animal Nutrition 19 (2024) 301–312

Contents lists available at ScienceDirect

Animal Nutrition

journal homepage: http://www.keaipublishing.com/en/journals/aninu/

Original Research Article

The dynamic distribution of the rectal microbiota in Holstein dairy calves provides a framework for understanding early-life gut health

Qi Huang, Fengtao Ma, Yuhang Jin, Duo Gao, Meinan Chang, Peng Sun*

State Key Laboratory of Animal Nutrition and Feeding, Institute of Animal Science, Chinese Academy of Agricultural Sciences, Beijing 100193, China

ARTICLE INFO

Article history:
Received 11 November 2023
Received in revised form
28 May 2024
Accepted 6 June 2024
Available online 3 August 2024

Keywords:
Calf
Rectal microbiota
Early life
Dynamic distribution

ABSTRACT

The posterior intestinal microbiota plays a vital role in the growth and health of Holstein dairy calves. However, its establishment and dynamic changes during early development remain unclear. The aim of this study was to investigate microbial colonization and development in the rectum of calves within the first 70 d after birth. Here, 96 rectal content samples were collected from 8 Holstein dairy calves at 12 time points and analyzed using 16S rRNA gene sequencing. The microbial alpha diversity increased with age. The bacterial community displayed a distinct dynamic distribution. The phylum Proteobacteria was replaced by Firmicutes and Bacteroidetes after d 3. The colonization process of bacterial genera in the rectum of neonatal calves can be divided into 2 periods: the colonization period (stage 1: d 1 and stage 2: d 3) and the stable period (stage 3: d 7–14, stage 4: d 21–42, and stage 5: d 49–70). The fermentation pattern and metabolic function changed from propionate fermentation dominated by *Shigella* to lactic acid fermentation dominated by *Lactobacillus*, *Blautia*, and *Oscillospira*. The stable period was more comprehensive and complete than the colonization period. This study revealed the dynamic changes in the posterior intestinal microbiota of Holstein dairy calves during early development. The transition period (d 7–14) was identified as a key stage for early nutritional intervention, as the abundance of *Lactobacillus* increased and the abundance of harmful bacteria (such as Proteobacteria and *Shigella*) decreased. This study provides a framework for understanding early-life gut health and offers theoretical guidance for future research on host–microbe interactions and early nutritional interventions. It is suggested that nutritional interventions based on microbial characteristics at different stages be implemented to improve calf growth performance and immune function, which may contribute to the reduction of diarrhea and other gastrointestinal disorders during dairy production.

1. Introduction

The gut microbiota is a complex and dynamic community that affects many host functions, such as metabolism, immunity, the gut barrier, and disease resistance (Fan et al., 2021; Valdes et al., 2018). The early colonization and development of the gut microbiota are among the most important factors for gut health, as they improve the microecological balance, increase nutrient absorption, control intestinal infection and regulate immune function (Arrieta et al., 2014; Ronan et al., 2021; Xiao et al., 2021). Specific microorganisms that are closely related to disease onset and progression are important targets for designing and evaluating intervention strategies to regulate the gut microbiota during early life (Choudhury et al., 2019). Ma et al. (2020) proposed that *Trueperella*, *Streptococcus*, *Dorea*, *Uncultured* Lachnospiraceae, *Ruminococcus 2*, and *Erysipelatoclostridium* were strongly correlated with the rate of diarrhea in calves and could be used as key targets for predicting diarrhea in young animals, with a prediction accuracy of up to 84.3%. Chen et al. (2022) suggested that some species of *Prevotella* might constitute the core microbiota of newborn and weaned calves, while *Muribaculaceae* may constitute the core microbiota of weaned calves to prevent diarrhea. They also proposed some

* Corresponding author.
E-mail address: sunpeng02@caas.cn (P. Sun).
Peer review under the responsibility of Chinese Association of Animal Science and Veterinary Medicine.

Production and Hosting by Elsevier on behalf of KeAi

https://doi.org/10.1016/j.aninu.2024.06.007

probiotics and biomarkers that could be used to prevent calf diarrhea and predict diarrhea risk.

Compared with adult animals, young animals are more prone to intestinal pathogen colonization and gastrointestinal diseases due to their immature gastrointestinal tract (GIT) and microbiota, especially during the period from birth to weaning (Kim et al., 2021; Quijada et al., 2020). The preweaning period is a critical period for the establishment and development of microbial communities within the intestines of calves (Luo et al., 2022). Therefore, understanding the early colonization and development patterns of the gut microbiota may help us to elucidate the relationship between the gut microbiota and host health and provide a reference for the development of new treatment methods (such as fecal microbiota transplantation, probiotics, and prebiotics).

However, there is limited research on the development of the gut microbiota in calves, and systematic dynamic analysis is lacking. Therefore, in the present study, the rectal microbiota community structure and diversity of Holstein dairy calves was evaluated within 70 d after birth and the dynamic distribution of the rectal microbiota was revealed. This study may provide a framework for understanding gut health during early life and offer theoretical guidance for future research on early host–microbe interactions and interventions to reduce diarrhea and other gastrointestinal disorders during dairy calf breeding.

2. Materials and methods

This study followed the principles of the Basel Declaration and the recommendations of the Chinese Academy of Agricultural Sciences Animal Care and Use Committee (Beijing, China). The experimental protocol was approved by the Ethics Committee of the Chinese Academy of Agricultural Sciences (IAS2019-62, Beijing, China).

2.1. Animal study and sample collection

Eight newborn Holstein female dairy calves with similar initial body weights (40.1 ± 0.87 kg) were randomly selected from the Beijing Dairy Cow Center (Beijing, China). Immediately after birth, the calves were removed from their dams and housed in individual pens (1.8 m length × 1.4 m width × 1.2 m height) to avoid cross-contamination. All the calves were fed 4 L of colostrum obtained from their respective dams from a bottle within 1 h after birth. From d 2 to 4, they were fed 1.5 L of raw milk 3 times a day (at 06:00, 14:00 and 18:00). From d 5 to 70, they were fed 4 L of raw milk twice a day (at 06:00 and 18:00). The raw milk, which was collected from healthy Holstein dairy cows on the farm, was heated to 60 °C, cooled to 38 to 39 °C and then fed to the calves. The granulated starter was purchased from the Feed Branch of Beijing Shounong Animal Science and Technology Development Co., Ltd. (Beijing, China), and fed to the calves beginning on d 3. All the calves received the same colostrum, raw milk, and starter concentrate. The nutrient compositions of the starter and milk are shown in Table 1. The amount of raw milk gradually decreased, and the calves were weaned at 70 d of age. Similar health management practices (nutrition, vaccinations, anthelmintic treatments, etc.) were applied for all calves that remained healthy and did not receive any additional antibiotics throughout the entire experimental period.

Calves were weighed biweekly to calculate average daily gain (ADG). Starter and milk intake and health checks were monitored and recorded every day. The dry matter (DM) intake of each calf associated with the starter and milk was also recorded, and the average daily starter intake and average daily feed intake were calculated. The starter was collected for the analysis of DM content (AOAC, 2005; method 930.15), crude protein (CP) (AOAC, 2000; method 976.05) and ether extract (EE) (AOAC, 2003; method 4.5.05) using the standard procedures of the Association of Official Analytical Chemists. The neutral detergent fiber (NDF) and acid detergent fiber (ADF) contents were determined as reported by Van Soest et al. (1991). Sodium sulfite and heat-stable α-amylase (Sigma A3306, Sigma–Aldrich) were used for NDF analysis. The contents of milk fat, milk protein, lactose, total solids and solids-not-fat in the milk were determined by a fully automated milk composition analyzer (MilkoScon FT6000, FOSS, Hillerød, Denmark).

A total of 96 rectal content samples were collected from the rectums of the calves on the mornings of d 1, 3, 7, 14, 21, 28, 35, 42, 49, 56, 63, and 70. Fresh rectal content samples (approximately 1.5 g/tube) were collected using sterile gloves and immediately placed into 2 mL DNase/RNase-free centrifuge tubes (Corning, NY, USA), which were snap-frozen in liquid nitrogen and then stored at −80 °C.

2.2. Extraction of rectal bacterial DNA

Rectal content samples were thawed, and bacterial genomic DNA was extracted from approximately 0.25 g of each sample using Fast DNA SPIN extraction kits (MP Biomedicals, Santa Ana, CA, USA)

Table 1
Ingredients of the starter, and nutrient levels of the starter and milk.

Starter ingredients	Content, % as-fed basis	Starter nutrient levels[3]	Content, %, DM basis	Milk composition	Content, % as-is basis
Corn	22.94	DM	89.0	Milk protein	3.25
Wheat bran	3.77	CP	24.5	Milk fat	4.02
Wheat middling	2.59	EE	1.68	Lactose	4.91
Soybean meal	20.35	Ash	7.75	TS	12.6
Flaked soybean	8.00	NDF	12.2	SNF	9.15
Rapeseed meal	5.00	ADF	4.85		
Flaked maize	10.0				
Sprayed corn bran	5.00				
DDGS	8.00				
Yeast culture[1]	3.00				
Soybean hull	5.35				
Molasses	2.00				
Premix[2]	4.00				

DDGS = distillers dried grains with solubles; DM = dry matter; CP = crude protein; EE = ether extract; NDF = neutral detergent fiber; ADF = acid detergent fiber; TS = total solids; SNF = solids-not-fat.
[1] Diamond V XP yeast culture supplement (Diamond V, Cedar Rapids, IA, USA).
[2] One kilogram of premix provided 530,000 IU vitamin A; 70,000 IU vitamin D; 800 mg vitamin E; 650 mg Cu; 3800 mg Fe; 3200 mg Zn; 2400 mg Mn; 85 mg I; 20 mg Se; and 8 mg Co.
[3] Analyzed value.

according to the manufacturer's instructions. The samples were centrifuged, and the pellet was resuspended. The process followed the FastPrep 24 (MP Biomedicals, Santa Ana, CA, USA) protocol. The concentration and purity of the extracted DNA were measured using a NanoDrop spectrophotometer (Thermo Fisher Scientific, Waltham, MA, USA), and the integrity of the DNA was assessed by 1% agarose gel electrophoresis to confirm successful DNA isolation. The DNA concentrations for all the samples are shown in Supplementary Table S1.

2.3. 16S rRNA gene amplicon sequencing

The V3 to V4 region of the bacterial 16S rRNA gene was amplified by PCR using the forward primer 338F (5′-ACTCCTACGGGAGGCAGCA-3′) and the reverse primer 806R (5′-GGACTACHVGGGTWTCTAAT-3′). The primers were tagged with sample-specific 7-bp barcodes for multiplex sequencing. The PCR program consisted of an initial denaturation step at 98 °C for 2 min, followed by 25 cycles of denaturation at 98 °C for 15 s, annealing at 55 °C for 30 s and extension at 72 °C for 30 s, and a final extension step at 72 °C for 30 s. The PCR mixture contained PrimeSTAR buffer (5 × , 4 μL), dNTPs (2.5 mmol/L, 2 μL), each primer (5 μmol/L, 0.8 μL), PrimeSTAR heat stress DNA polymerase (TaKaRa, Dalian, China; 0.4 μL), and template DNA (20 ng) in a final volume of 20 μL. Each sample was analyzed in triplicate. The amplicons were purified using a DNA Gel Extraction Kit (AxyPrep) and sequenced on an Illumina NovaSeq sequencing platform to obtain 250 bp paired-end reads at Personalbio Company (Shanghai). The raw sequencing data were deposited in the NCBI Sequence Read Archive (SRA) database under the accession number SRP320638 (https://www.ncbi.nlm.nih.gov/sra/?term=SRP320638).

2.4. Bioinformatics analysis

Microbiome bioinformatics analyses were performed with Quantitative Insights Into Microbial Ecology (QIIME 2-2019.4) software with slight modifications according to official tutorials (https://docs.qiime2.org/2019.4/tutorials/) (Bolyen et al., 2018). Briefly, raw sequence data were demultiplexed using the demux plugin, followed by primer trimming with the cutadapt plugin (Kechin et al., 2017). The sequences were then quality filtered, denoised, merged and made chimera free using the DADA2 plugin (Callahan et al., 2016). Nonsingleton amplicon sequence variants (ASV) were aligned with MAFFT (Katoh et al., 2002) and used to construct a phylogenetic tree with FastTree 2 (Price et al., 2010). Alpha diversity indices (observed ASV, Chao1, Shannon, and Simpson indices) and beta diversity indices (weighted UniFrac) (Lozupone et al., 2007) were estimated using the diversity plugin. Taxonomy was assigned to ASV using the classify-sklearn Naïve Bayes taxonomy classifier in the feature classifier plugin (Bokulich et al., 2018) based on the Greengenes reference database (McDonald et al., 2012). Beta diversity was visualized using weighted UniFrac principal coordinates analysis (PCoA) (Ramette, 2007), and the different sites were statistically compared using analysis of similarity (ANOSIM) based on weighted UniFrac in the Vegan package in R (Lozupone and Knight, 2005; Warton et al., 2012).

The linear discriminant analysis effect size (LEFSe) (Segata et al., 2011) and random forest regression (Breiman, 2001) were performed to identify differentially abundant taxa between groups using the LEfSe tool and randomForest package, with a default filter value of 3 for the linear discriminant analysis (LDA) score. Microbial functions were predicted by phylogenetic analysis of communities through reconstruction of unobserved states (PICRUSt2) based on MetaCyc databases (Caspi et al., 2016; Douglas et al., 2020). Differential analysis of the MetaCyc metabolic pathways was performed using the metagenomeSeq package in R. The correlation between bacterial taxa and MetaCyc metabolic pathways was evaluated by the Pearson correlation test. Finally, the coexpression network graphs of bacterial taxa and metabolic pathways ($|r| > 0.9$, adjusted P-value <0.01) were visualized and analyzed using Cytoscape software (version 3.8.0). Time-series analysis was performed by Short Time-Series Expression Miner (STEM) (Ernst and Bar-Joseph, 2006).

2.5. Statistical analysis

The growth performance was analyzed using one-way ANOVA followed by Tukey's test in SPSS statistics 26.0 software (IBM; USA). A value of $P < 0.05$ was regarded as statistically significant. Differences in alpha diversity indices and relative abundances of rectal bacterial phyla and genera among different days of age were assessed using the nonparametric Kruskal–Wallis test with Dunn's post hoc test for multiple comparisons in SPSS statistics 26.0 software (IBM; USA). Two-sided Welch's test and Benjamini–Hochberg (BH) false discovery rate (FDR) correction were used for 2-group analysis. ANOVA with the Tukey–Kramer test and BH correction were chosen for multiple-group analysis. The significance was assessed based on an FDR adjusted $P < 0.05$. The relationships among the various microbial and MetaCyc metabolic pathways were analyzed using Pearson correlation coefficients.

3. Results

3.1. Growth performance

The initial average body weight of the 8 dairy calves was 40.1 kg. As the calves grew, starter intake and total feed intake significantly increased (Table 2, $P < 0.001$), resulting in a corresponding increase in the ADG of dairy calves ($P < 0.001$). The final body weight of the dairy calves reached 95.6 kg. Additionally, the feed-to-gain ratio decreased gradually and was greater during the first 2 weeks than during the other periods ($P < 0.001$).

3.2. Dynamic changes in the rectal bacterial microbiota of calves

In total, 6,120,883 high-quality sequences were obtained from 96 rectal samples, with an average of 63,759 ± 1584.8 (mean ± SEM)

Table 2
The dynamic distributions of growth performance of preweaning Holstein dairy calves.

Item	Age					SEM	*P*-value
	Day 1–14	Day 15–28	Day 29–42	Day 43–56	Day 57–70		
Average daily gain, g/d	453^{d}	660^{c}	811^{bc}	956^{ab}	1083^{a}	39.4	<0.001
Starter intake, g DM/d	12.3^{e}	130^{d}	303^{c}	472^{b}	718^{a}	41.3	<0.001
Total feed intake, g DM/d	981^{e}	1097^{d}	1288^{c}	1446^{b}	1687^{a}	41.8	<0.001
Feed-to-gain ratio	2.25^{a}	1.71^{b}	1.60^{b}	1.54^{b}	1.57^{b}	0.06	<0.001

$^{a, b, c, d, e}$ Values with different superscripts within a row indicate a significant difference ($P < 0.05$).

sequences per sample (Supplementary Table S2). During the whole experimental period, the Shannon index decreased from 1 to 3 d but then gradually increased, albeit with fluctuations, and stabilized at 50 d (Fig. 1A). A total of 48,631 ASV were identified from all the rectal content samples, of which 46 were present in all groups and defined as core ASV (Fig. 1B).

At the phylum level, the dominant microbial communities from d 1 to 70 were Proteobacteria, Firmicutes, and Bacteroidetes (Fig. 1C). The relative abundance of Proteobacteria was greater than 60% on d 1 and 3, but decreased significantly from d 35 to 70 ($P < 0.05$; Fig. 1D). In contrast, Firmicutes and Bacteroidetes increased gradually after 7 d of age and replaced Proteobacteria as the dominant phylum. The relative abundance of Bacteroidetes on d 28, 49, 56 and 63 was significantly greater than that on d 1 ($P < 0.05$; Fig. 1D). The relative abundance of Firmicutes ranged from 47.78% to 82.98% after 7 d of age (Fig. 1D and Supplementary Table S3). Additionally, the relative abundance of Actinobacteria on d 7 (3.65%) and 14 (4.27%) increased by 24-fold and 28-fold compared with that on d 3 (0.15%), respectively, and then stabilized at approximately 1% (Fig. 1D and Supplementary Table S3).

Of the bacterial genera identified across all the fecal samples, 14 genera had a relative abundance >1% in at least 60% of the fecal samples on a single day. These genera were Bacteroidaceae_*Bacteroides*, *Faecalibacterium*, *Shigella*, *Lactobacillus*, *Blautia*, *Prevotella*, *[Prevotella]*, *Dorea*, *Butyricicoccus*, *Oscillospira*, *Collinsella*, *[Ruminococcus]*, *Streptococcus*, and *Parabacteroides* (Fig. 1E and F and Supplementary Table S4). At the genus level, *Shigella* was the dominant genus during the first 3 d after birth, while *Faecalibacterium*, Bacteroidaceae_*Bacteroides*, *Lactobacillus*, and *Prevotella* were the predominant genera after d 7 (Fig. 1E). The relative abundance of *Shigella* on d 1 (39.41%) and 3 (66.93%) was greater than that on d 35, 49, 56, 63 and 70 ($P < 0.05$). The abundances of Bacteroidaceae_*Bacteroides* and *Faecalibacterium* were greater at approximately d 7 to 63 than at d 1, although there were fluctuations, and then decreased toward the end of the trial. The relative abundance of *Lactobacillus* on d 7, 14 and 21 (20.05% to

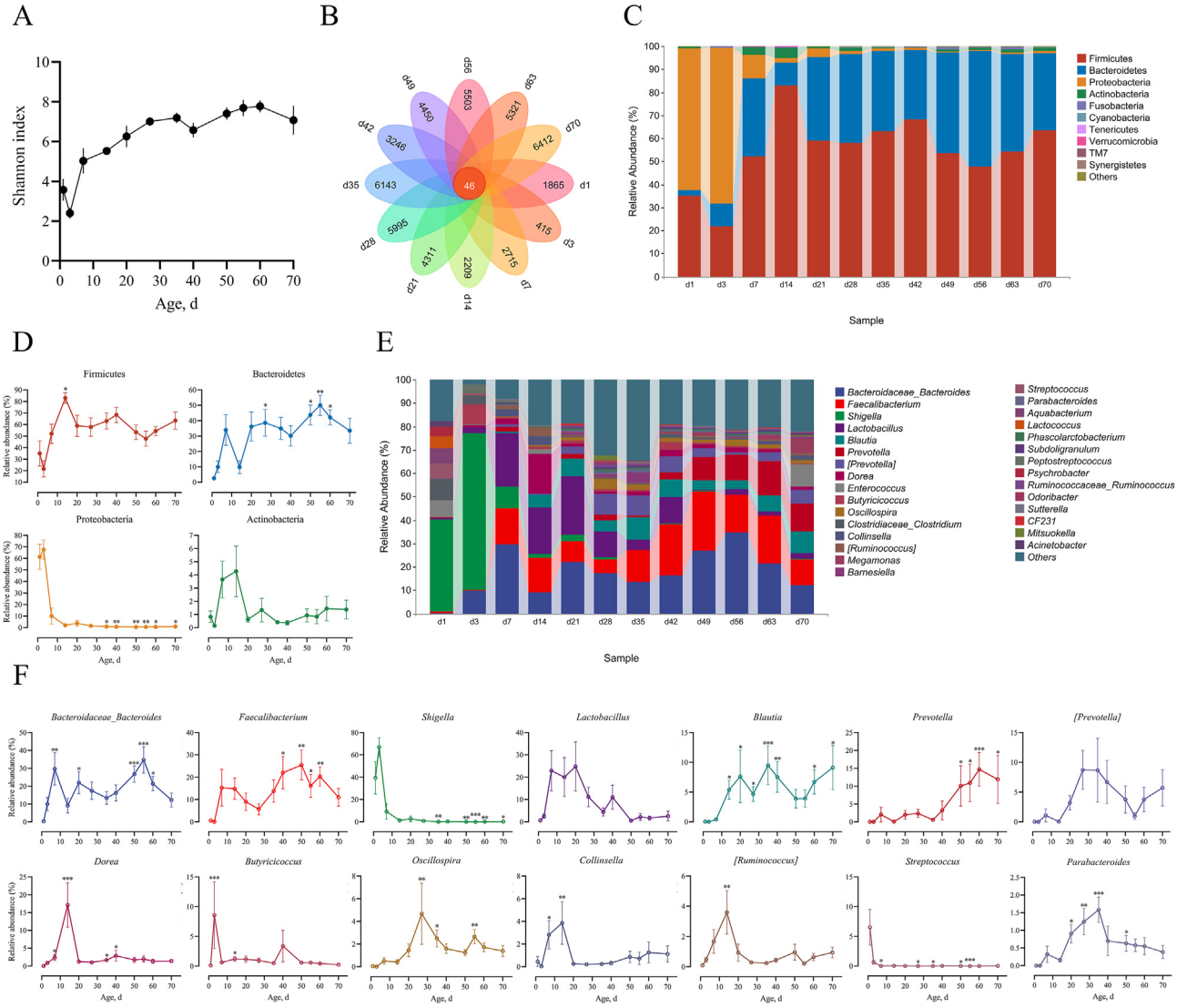

Fig. 1. Dynamic changes in alpha diversity metrics (Shannon index) (A); Venn diagram of amplicon sequence variants (ASV) at different ages (B); relative abundance of the top 10 bacterial phyla across ages (C); the major bacterial phyla at different ages are expressed as the median and SEM (D); relative abundance of the top 30 bacterial genera across ages (E); and the major bacterial genera of the different ages are expressed as medians and SEM (F). Only the phyla and genera with a relative abundance >1% in at least 60% of the samples at any single age are shown. A relative abundance significantly different from that of d 1 is indicated by *$P < 0.05$, **$P < 0.01$, and ***$P < 0.001$ according to the nonparametric Kruskal–Wallis test with Dunn's post hoc test for multiple comparisons.

24.84%) suddenly increased by 7- to 9-fold compared with that on d 3 (2.59%) and then decreased.

Remarkably, the relative abundance of *Dorea* was the highest (17.14%) on d 14, while that of *Prevotella* was the highest on d 63, and that of *Blautia* increased after 7 d of life and then varied, peaking on d 35. Compared to d 1, the relative abundance of *Butyricicoccus* increased and then decreased sharply ($P < 0.001$) on d 3. The abundances of *Oscillospira*, *Collinsella*, *[Ruminococcus]* and *Parabacteroides* peaked at different time points (14–35 d) during the experiment ($P < 0.01$), but they all showed similar patterns of first increasing and then decreasing. *Streptococcus* was different from all the other genera, as its initial relative abundance decreased dramatically on d 7 ($P = 0.022$), and it never recovered.

3.3. Composition and distribution of bacterial genera

The 30 most abundant genera were analyzed via a hierarchical clustering heatmap and divided into 5 clusters (Fig. 2A). Among these genera, *Enterococcus, Clostridium, Streptococcus, Acinetobacter, Lactococcus, Aquabacterium,* and *Psychrobacter* in the first cluster predominated on d 1; *Shigella, Butyricicoccus,* and *Peptostreptococcus* in the second cluster predominated on d 3; *Lactobacillus, Dorea, Collinsella,* and *[Ruminococcus]* in the 3rd cluster predominated from d 7 to 14; *Barnesiella, Mitsuokella, Phascolarctobacterium, Subdoligranulum, Oscillospira, Odoribacter, [Prevotella], Parabacteroides, Blautia,* and *CF231* in the 4th cluster predominated from d 21 to 42; and *Prevotella, Megamonas, Coprococcus, Bacteroides, Faecalibacterium,* and *Sutterella* in the 5th cluster predominated from d 49 to 70. The STEM analysis identified a significant module, including *Blautia, [Prevotella], Barnesiella, Parabacteroides,* and *Odoribacter*, all belonging to the 4th cluster ($P = 0.007$; Fig. 2B). Based on the distribution of the high-abundance bacterial genera, the entire experimental period was divided into 5 stages, and PCoA was used to visualize the bacterial distribution of each cluster (Fig. 2C; d 1, d 3, d 7–14, d 21–42, and d 49–79).

The main bacterial genera that changed dynamically with age were identified using random forest regression (Fig. 3A). The 30 most abundant bacterial genera belonged to 4 phyla: Firmicutes (17 genera), Bacteroidetes (5 genera), Proteobacteria (5 genera), and Actinobacteria (3 genera) (Fig. 3B). The PCoA and ANOSIM showed that the 5 stages were distributed in 2 clusters, each corresponding to an age period (Fig. 4 A, B and Table 3; colonization period vs. stable period, $R = 0.830$ and $P = 0.001$). The colonization period included stages 1 and 2 (d 1–3), and the stable period included stages 3 to 5 (d 7-70).

The Kruskal–Wallis test and LEfSe analysis using LDA were performed to further investigate the differences between samples, and an LDA score ≥3 was observed for the colonization period and stable period (Fig. 4C). This threshold ensured that only informative taxa were compared and that most rare taxa were eliminated. During the stable period, the bacteria mainly belonged to the Proteobacteria, including the genera *Brevundimonas, Craurococcus, Sphingomonas, Aquabacterium, Pelomonas, Arsenophonus, Shigella, Acinetobacter, and Psychrobacter.* In addition, the abundances of *Aerococcus, Alkalibacterium, Enterococcus, Lactococcus, Streptococcus,* and *Clostridium* of Firmicutes, as well as *Flavobacterium* and *Sufflavibacter* of Bacteroidetes, increased during the stable period. During the colonization period, the bacteria mainly belonged to the phyla Firmicutes, Actinobacteria, and Bacteroidetes. At the genus level, the abundances of *Ruminococcus, Faecalibacterium, Oscillospira, Subdoligranulum, Megamonas, Phascolarctobacterium, [Ruminococcus], Blautia, Dorea, Lactobacillus, Collinsella, Barnesiella, [Prevotella], Bacteroides, Parabacteroides, and Prevotella* were greater during the stable period.

3.4. Microbial function prediction and intestinal metabolic pathways

A functional analysis of the fecal bacterial microbiota of calves between the stable period and the colonization period was performed using PICRUSt2, and the abundance of metabolic pathways was estimated with the MetaCyc database as a reference. The functional abundance statistics revealed that most microbial functions were involved biosynthesis and degradation/utilization/assimilation (Fig. 5A). Biosynthetic processes had a

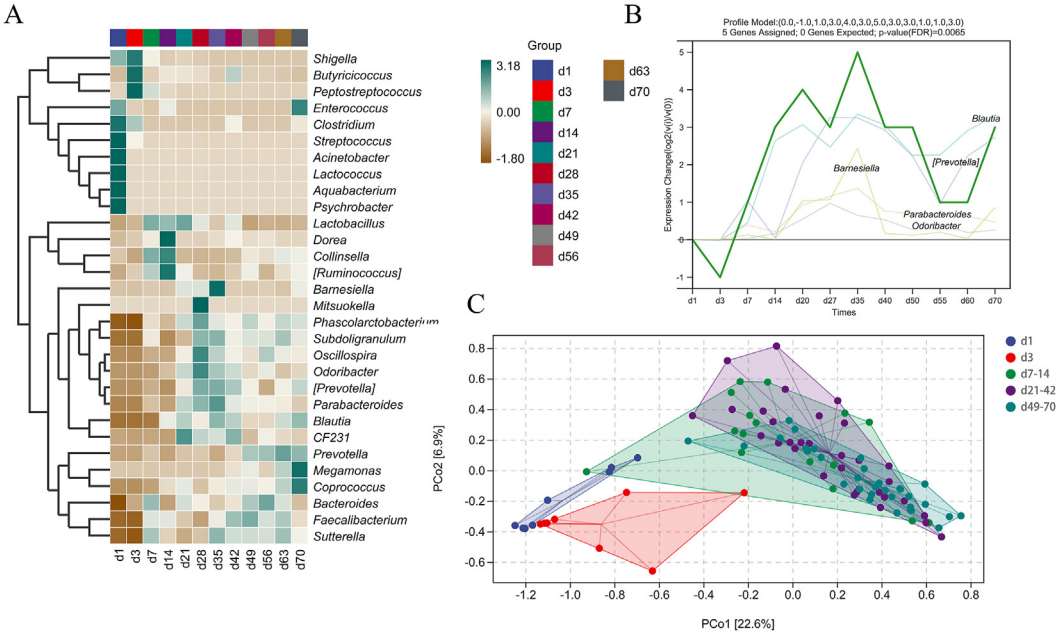

Fig. 2. Heatmap of species abundance clustering for the 30 most abundant genera (A); time-series analysis of the top 30 genera by short time-series expression minus (STEM) analysis (B); and principal coordinate analysis (PCoA) of the bacterial microbiota across different stages (C).

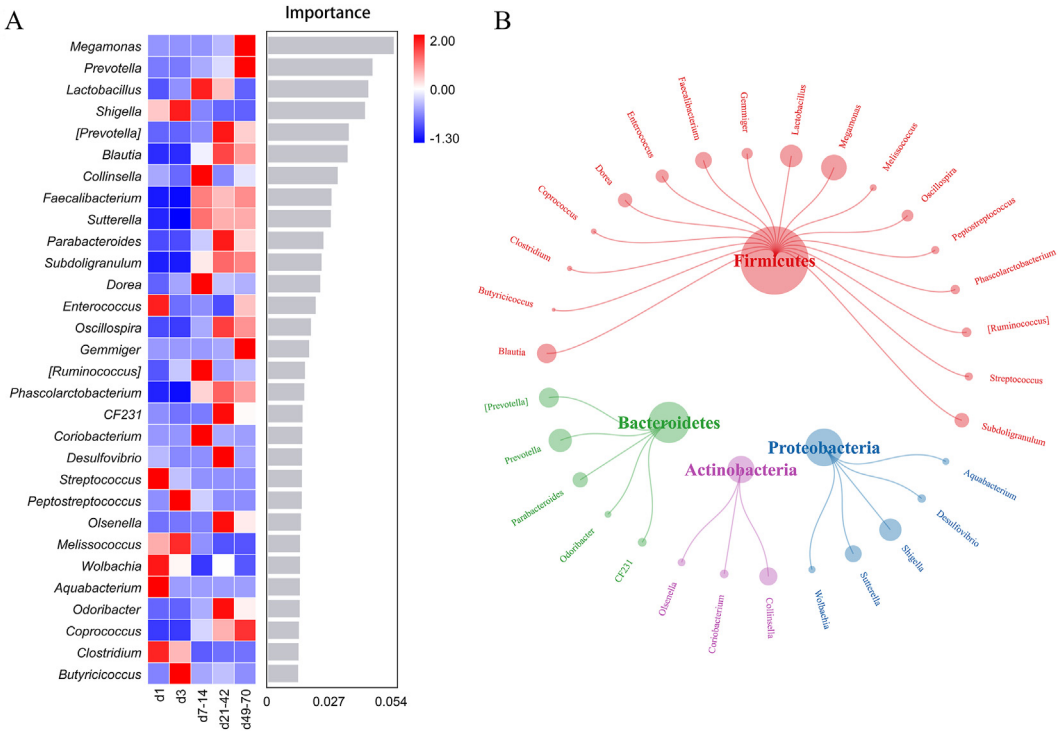

Fig. 3. Heatmap of the 30 most abundant genera among 5 stages ranked by importance to the accuracy of the random forest regression model and the clusters they formed based on their relative abundance (A); and the affiliation network diagram (B).

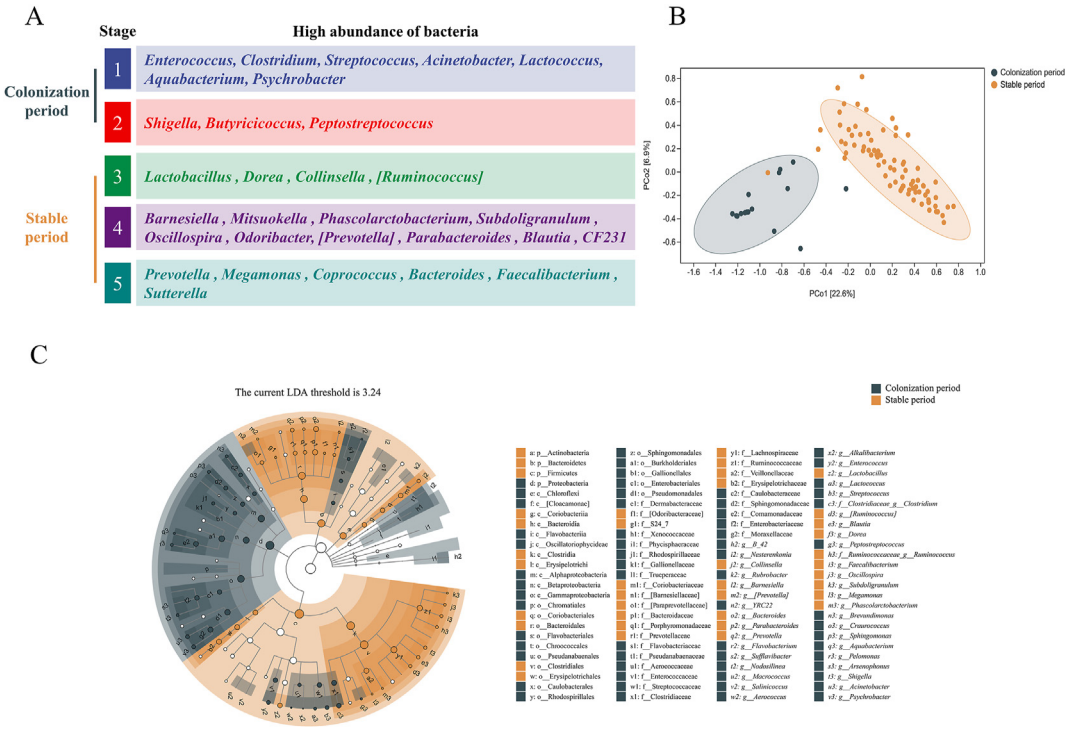

Fig. 4. Schematic diagram of the genera of high abundance bacteria at different stages (A); principal coordinate analysis (PCoA) of the bacterial microbiota across the colonization period and stable period (B); and Linear discriminant analysis effect size (LEfSe) cladogram (C).

significantly greater abundance than did the other metabolic pathways. The main biological pathways included amino acid biosynthesis, nucleoside and nucleotide biosynthesis, cofactors, prosthetic groups, electron carriers, vitamin biosynthesis, fatty acid and lipid biosynthesis, and carbohydrate biosynthesis. Moreover, carbohydrate degradation was the main biological pathway involved in the processes of degradation/utilization/assimilation.

Table 3
Analysis of similarity (ANOSIM) of rectal microbiota beta diversity at different stages[1].

Age	Age	*R*-value	*P*-value
Day 1	Day 3	0.204	0.018
Day 1	Day 7–14	**0.731**	**0.001**
Day 1	Day 21–42	**0.937**	**0.001**
Day 1	Day 49–70	**0.960**	**0.001**
Day 3	Day 7–14	**0.618**	**0.001**
Day 3	Day 21–42	**0.830**	**0.001**
Day 3	Day 49–70	**0.901**	**0.001**
Day 7–14	Day 21–42	0.141	0.013
Day 7–14	Day 49–70	0.370	0.001
Day 21–42	Day 49–70	0.119	0.001
Day 1–3	Day 7–70	**0.831**	**0.001**

[1] The numbers in bold indicate *R*-values > 0.5 and *P*- values < 0.05. The fecal microbiota of the two age groups were considered completely different at $R > 0.75$, different at $0.5 < R < 0.75$, tended to be different at $0.3 < R < 0.5$, and did not differ at $R < 0.3$.

MetagenomeSeq analysis was used to identify metabolic pathways that differed significantly between groups (logFC >2 or logFC < −2, and adjusted $P < 0.05$). A total of 110 metabolic pathways (54 upregulated and 56 downregulated pathways) exhibited significant differences between the stable period and the colonization period. A total of 41 metabolic pathways related to carbohydrate and protein metabolism were selected, which included volatile fatty acid (VFA) production and degradation, CH_4 production, lactic acid production, amino acid degradation and production, and carbohydrate metabolism (Fig. 5B and Table 4).

3.5. Coexpression network graphs of bacterial genera and metabolic pathways

The link between bacterial genera and function was investigated, which could serve as a foundation for further investigations of dynamic changes in the fecal bacterial microbiota of calves. A coexpression network of bacterial genera and metabolic pathways was constructed, and several modules that were clustered in this coexpression network were identified. The genera identified via LEfSe analysis (LDA score ≥3) and the metabolic pathways related to carbohydrate and protein metabolism were used as a dataset, and correlations were calculated via Pearson correlation analysis (Supplementary Table S5). Then, only robust (|r| > 0.9) and statistically significant (adjusted *P*-value <0.01) correlations were retained for the coexpression network graphs.

A total of 72 differentially positive relationship pairs were identified and divided into 6 coexpression modules (Fig. 6). The first coexpression module was associated with the sucrose biosynthesis pathway in carbohydrate metabolism (sucrose biosynthesis III [PWY-7347]; sucrose biosynthesis I [SUCSYN-PWY]) (from photosynthesis) and was positively correlated with 21 bacterial genera, including *Psychrobacter, Aerococcus, Alkalibacterium, Brachybacterium, Craurococcus, YRC22, Nesterenkonia, Sufflavibacter, Macrococcus, Skermanella, Comamonas, Aequorivita, Ornithobacterium, Bizionia, Salinicoccus, Arsenophonus, Truepera, Nodosilinea, Staphylococcus, Thiocystis,* and *Aeromonas.* The second coexpression module was involved in VFA (propionate) degradation (2-methylcitrate cycle II [PWY-5747] and 2-methylcitrate cycle I [PWY0-42]), carbohydrate metabolism (glucose and glucose-1-phosphate degradation [GLUCOSE1PMETAB-PWY]), amino acid degradation (superpathway of ornithine degradation [ORNDEG-PWY] and L-arginine degradation II [AST-PWY]), and lactic acid production (superpathway of methylglyoxal degradation [METHGLYUT-PWY]) and was positively correlated with only 1 bacterial genus, *Shigella.* The 3rd coexpression module included carbohydrate metabolism (L-arabinose degradation IV [PWY-7295]; glucose degradation (oxidative) [DHGLUCONATE-PYR-CAT-PWY]; starch degradation III [PWY-6731]), amino acid degradation (superpathway of L-arginine, putrescine, and 4-aminobutanoate degradation [ARGDEG-PWY]; superpathway of L-arginine and L-ornithine degradation [ORNARGDEG-PWY]), and CH_4 production (factor 420 biosynthesis [PWY-5198]) and was

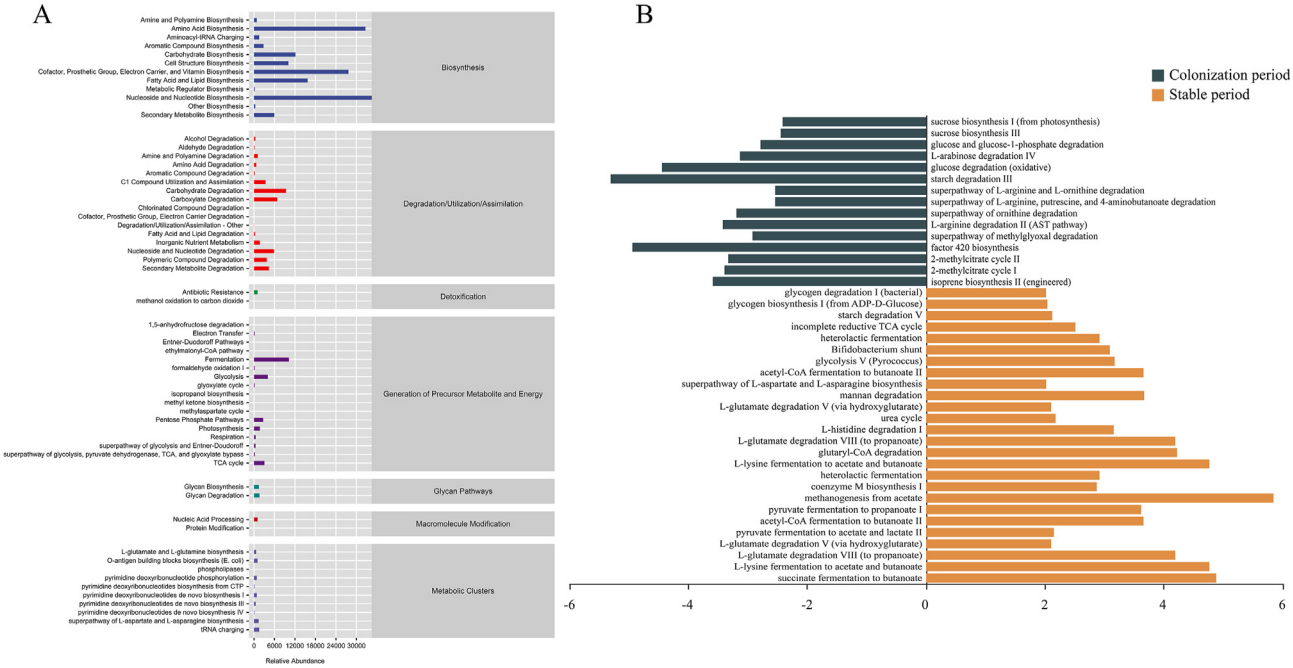

Fig. 5. The abundances of the differential metabolic pathways based on the MetaCyc database (A). The abscissa is the abundance count of the classification, the ordinate is the functional pathway of MetaCyc's second classification level, and the rightmost is the first-level classification to which this pathway belongs. Histogram of metabolic functions related to carbohydrate and protein metabolism in positive and negative coordinates (logFC >2 or logFC < −2, and adjusted $P < 0.05$) (B). FC = fold change.

Table 4
MetaCyc predicted microbial metabolic functions related to carbohydrate metabolism and protein metabolism.

Function	Pathway	logFC	SE	Adjusted *P*-values
VFA production	Succinate fermentation to butanoate	4.88	1.25	0.002
	L-lysine fermentation to acetate and butanoate	4.77	0.551	<0.001
	L-glutamate degradation VIII (to propanoate)	4.19	0.859	<0.001
	L-glutamate degradation V (via hydroxyglutarate)	2.10	0.591	0.004
	Pyruvate fermentation to acetate and lactate II	2.15	0.601	0.004
	Acetyl-CoA fermentation to butanoate II	3.66	1.05	0.005
CH_4 production	Methanogenesis from acetate	5.85	1.33	<0.001
	Coenzyme M biosynthesis I	2.87	0.789	0.003
Lactic acid production	Heterolactic fermentation	2.92	1.11	0.025
Amino acid degradation	L-lysine fermentation to acetate and butanoate	4.77	0.551	<0.001
	Glutaryl-CoA degradation	4.22	1.29	0.007
	L-glutamate degradation VIII (to propanoate)	4.19	0.859	<0.001
	L-histidine degradation I	3.16	1.42	0.057
	Urea cycle	2.18	1.72	0.298
	L-glutamate degradation V (via hydroxyglutarate)	2.10	0.591	0.004
Amino acid production	Mannan degradation	3.67	1.51	0.038
	Superpathway of L-aspartate and L-asparagine biosynthesis	2.02	0.603	0.006
Carbohydrates metabolism	Acetyl-CoA fermentation to butanoate II	3.66	1.05	0.005
	Glycolysis V (Pyrococcus)	3.17	1.00	0.007
	Bifidobacterium shunt	3.09	1.12	0.018
	Heterolactic fermentation	2.92	1.11	0.025
	Incomplete reductive TCA cycle	2.51	0.898	0.017
	Starch degradation V	2.12	0.588	0.003
	Glycogen biosynthesis I (from ADP-D-glucose)	2.04	0.607	0.006
	Glycogen degradation I (bacterial)	2.02	0.576	0.004
VFA production	Isoprene biosynthesis II (engineered)	−3.59	1.58	0.050
VFA degradation	2-Methylcitrate cycle I	−3.39	1.11	0.010
	2-Methylcitrate cycle II	−3.33	1.06	0.008
CH_4 production	Factor 420 biosynthesis	−4.95	1.28	0.002
Lactic acid production	Superpathway of methylglyoxal degradation	−2.92	1.09	0.022
Amino acid degradation	L-arginine degradation II (AST pathway)	−3.42	1.24	0.018
	Superpathway of ornithine degradation	−3.19	0.412	<0.001
	Superpathway of L-arginine, putrescine, and 4-aminobutanoate degradation	−2.54	0.585	<0.001
	Superpathway of L-arginine and L-ornithine degradation	−2.54	0.585	<0.001
Carbohydrates metabolism	Starch degradation III	−5.31	0.763	<0.001
	Glucose degradation (oxidative)	−4.45	1.09	0.001
	L-arabinose degradation IV	−3.13	1.33	0.044
	Glucose and glucose-1-phosphate degradation	−2.79	1.12	0.034
	Sucrose biosynthesis III	−2.45	1.30	0.111
	Sucrose biosynthesis I (from photosynthesis)	−2.42	1.28	0.111

FC = fold change; VFA = volatile fatty acid; AST = arginine succinyltransferase.

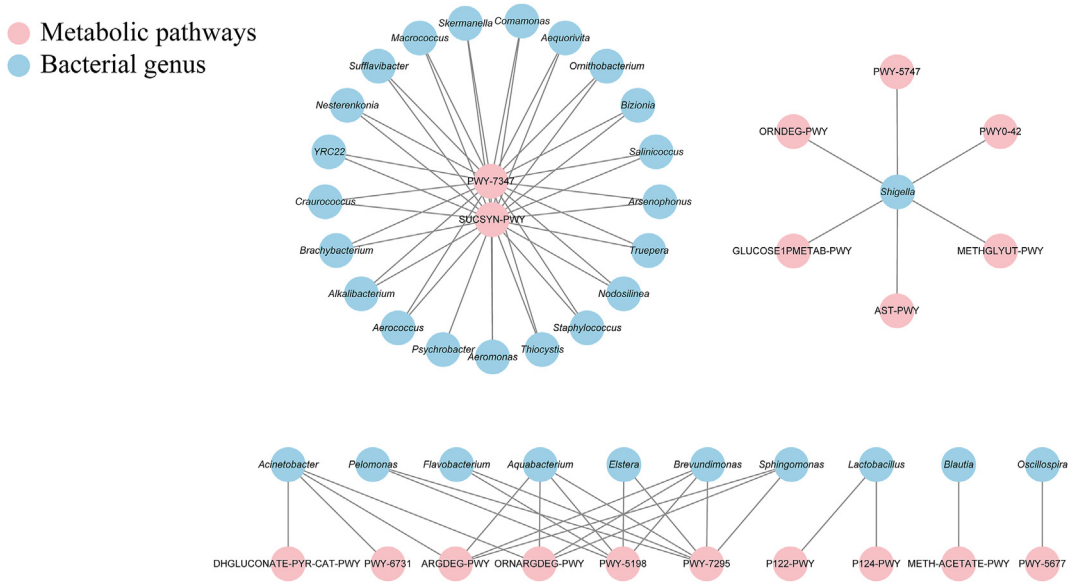

Fig. 6. Linear discriminant analysis effect size (LEfSe) analysis of genera (linear discriminant analysis score ≥3) and the metabolic pathways related to the carbohydrate and protein metabolism coexpression network diagram.

positively correlated with 7 bacterial genera, including *Aquabacterium, Brevundimonas, Flavobacterium, Pelomonas, Sphingomonas, Elstera, and Acinetobacter.* The 4th coexpression module was involved in carbohydrate metabolism and lactic acid production (*Bifidobacterium* shunt [P124-PWY]; *heterolactic* fermentation [P122-PWY]) and was positively correlated with *Lactobacillus.* The 5th coexpression module was associated with CH_4 production (methanogenesis from acetate [METH-ACETATE-PWY]) and showed a positive correlation with *Blautia.* The 6th coexpression module was involved in VFA production (succinate fermentation to butanoate [PWY-5677]) and showed a positive correlation with *Oscillospira.*

4. Discussion

Birth weight and ADG before weaning are important indicators of calf health status. The calves' body weights ranged from 37.9 to 44.0 kg at birth, which met the national standard of the People's Republic of China (GB/T 3157-2023) of not being lower than 36.0 kg. At 70 d of age, the calves' body weights ranged from 88.0 to 104 kg, with an ADG of 792 g/d. These values were consistent with the statistics of the United States Department of Agriculture Animal and Plant Health Inspection Service (USDA, 2021). These results suggest that the growth performance and health status of the calves in this study were similar to those of most calves in China and abroad.

In this study, the longitudinal changes in bovine fecal microbiota development during preweaning were evaluated. Sequencing of the 16S rRNA gene was used to analyze the microbial structure, composition, significantly enriched bacteria, and potential functions. The period from birth to weaning is a critical period for intestinal microbiota colonization and development, and its microbial communities show obvious temporal changes. The bacterial richness and diversity of preweaning calves generally increase with age, but within 7 d after birth, the bacterial richness declines and rapidly recovers (Dill-McFarland et al., 2017; Li et al., 2019; Rey et al., 2014; Yeoman et al., 2018). Our study revealed that the Shannon index of rectal microbes in preweaning calves increased significantly with age. This was consistent with the findings of Klein-Jöbstl et al. (2019) and Chen et al. (2022) on bacterial richness. Previous studies suggested that the preruminant GIT was first colonized by facultative anaerobes, including *Escherichia coli*, *Streptococcus*, and *Clostridium perfringens*, which colonize calves within 8 h after birth. As the calves grow older, the intestinal oxygen is depleted, and the abundances of facultative anaerobes, such as *Lactobacillus* and *Bacteroides*, are reduced, creating anaerobic conditions for obligate anaerobic gut microbiota (Jordan, 1976; Jost et al., 2012). This may be an important reason for the decrease in the number of microbes on d 3.

The dominant phyla in the rectal microbiota before weaning were Firmicutes, Bacteroidetes, Proteobacteria, and Actinobacteria, which was consistent with previous studies on the core microbiota in the bovine gut at different ages (Bi et al., 2021; Jami et al., 2013; Malmuthuge et al., 2019). A previous study reported that the enrichment of Proteobacteria in the gut, including Enterobacteriaceae, indicates an imbalanced or unstable microbial community structure or a disease state of the host (Shin et al., 2015). Many metabolic and inflammatory diseases are associated with the phylum Proteobacteria, a major phylum of gram-negative bacteria that increases the level of lipopolysaccharide endotoxin in the blood, decreases the number of intestinal barrier cells, and increases intestinal permeability (Cani et al., 2007; Rizzatti et al., 2017). In our study, Proteobacteria were abundant 3 d after birth and then decreased rapidly. *Shigella*, belonging to Enterobacteriaceae, showed the same changes as did the phylum Proteobacteria. It is a gram-negative invasive enteropathogenic bacterium that causes rupture, invasion, and inflammatory destruction of the colonic epithelium, leading to bacillary dysentery. Diarrhea is one of the most important health problems in young calves, especially during the first month after birth, and it is associated with a high abundance of harmful bacteria (Ma et al., 2020; Pempek et al., 2019). Chang et al. (2020) reported that calves with a high diarrhea rate had a greater abundance of Proteobacteria. One possible reason for this may be the absence of differentiated B cells and IgA production deficiency at 3 d after birth, which increases the susceptibility of calves to infection (Mirpuri et al., 2014; Rizzatti et al., 2017). Another possible reason may be the upregulation of PWY-722 (nicotinate degradation I), which produces fumarate as the final metabolite, during the colonization period. Fumarate is a component of fumarate and nitrate reduction (FNR), which is essential for the virulence of *Shigella* (Marteyn et al., 2010; Vergara-Irigaray et al., 2014). This suggests that some interventions, such as facilitating B-cell differentiation and IgA production or blocking the pathway of PWY-722 or the FNR, could modulate immunity and weaken some harmful bacteria (such as Proteobacteria and *Shigella*) one week after birth.

Megamonas, Prevotella and *Lactobacillus* were the most important genera in the random forest analysis. *Megamonas* and *Prevotella* were the most abundant genera in stage 5, while *Lactobacillus* was one of the most abundant genera in stage 3. *Megamonas* and *Prevotella* are Firmicutes that mainly ferment various carbohydrates and produce VFA, which are important for energy supply, rumen development and immune function (Nuli et al., 2019; Stevenson and Weimer, 2007; Xue et al., 2020). The high abundance of *Megamonas* and *Prevotella* during stage 5 may reflect the maturity and stability of the calf intestinal microbiota. *Lactobacillus* is a member of the Firmicutes and mainly uses lactose or other monosaccharides for fermentation, producing lactic acid, inhibiting the growth of harmful bacteria, maintaining the balance of intestinal pH, and promoting the establishment of the intestinal mucosal barrier (Cheirsilp et al., 2003; Liu et al., 2019; Vassallo et al., 2015). Studies have shown that *Lactobacillus* colonized 1 d after birth and then dominated in all regions of the GIT tested in the first week (Smith, 1965). The high abundance of *Lactobacillus* during stage 3 may be related to the dynamic changes in the calf intestinal microbiota because on d 4 after birth, with the feeding of the granulated starter and the adaptation of the digestive system, the intestinal microbiota underwent a transition period. During this period, the abundance of *Lactobacillus* increased, which gradually decreased the abundance of harmful bacteria (such as Proteobacteria and *Shigella*). This suggests that colonization by these genera during stage 3 (*Lactobacillus, Dorea, Collinsella,* and *[Ruminococcus]*) in the gut of young calves might facilitate the establishment of a functional gut and maintain the stability of the gut microbiota (Cascone et al., 2021; Liu et al., 2020; Sokol et al., 2017; Tian et al., 2019). Similarly, Schwaiger et al. (2022) showed that a greater abundance of diarrheal pathogens and the restricted development of *Lactobacillus* can cause intestinal dysbiosis, which is conducive to the onset of diarrhea in newborn calves. Therefore, strict management and appropriate preventive measures must be provided during early life, and nutritional interventions that promote the colonization of beneficial microbes, such as *Lactobacillus* and *Bifidobacterium* (such as galacto-oligosaccharide (Chang et al., 2022), zinc oxide (Chang et al., 2020), and zinc methionine (Yu et al., 2024), may be key to preventing and controlling the onset of diarrhea and other intestinal diseases.

During the colonization period, VFA production and degradation were mainly related to propionate. During the stable period, the number of metabolic pathways related to VFA production and degradation increased, and these pathways were mainly related to

acetate, butyrate and lactic acid. Acetate and butyrate are the main sources of energy for intestinal epithelial cells, and butyrate modulates the immune response, improving intestinal barrier function by increasing colonic mucin and tight junctions (Gonzalez et al., 2019; Wang et al., 2022; Xu et al., 2016). Interestingly, compared with those identified during the colonization period, there were no metabolic pathways associated with VFA degradation identified during the stable period, which means that in the early stages of life, in addition to meeting the energy needs of the host, part of the propionate produced by fermentation was degraded as a carbon source and energy for microorganisms. Among the metabolic pathways associated with amino acid metabolism, amino acid degradation in the stable period was more related to VFA production, and metabolic pathways related to amino acid biosynthesis were also more abundant during the stable period than during the colonization period (mannan degradation and the superpathway of L-aspartate and L-asparagine biosynthesis). In addition, from the perspective of the number of enriched metabolic pathways, whether protein metabolism or carbohydrate metabolism, the stable period was more comprehensive and complete than the colonization period.

Association analysis revealed that propionate production and degradation in calves during the colonization period were closely related to *Shigella*, while acetate and butyrate production during the stabilization period were closely related to *Lactobacillus, Blautia,* and *Oscillospira*. This suggested a shift in the fermentation pattern during calf development, from a propionate fermentation pattern dominated by *Shigella* in the colonization period to a lactic acid fermentation pattern dominated by *Lactobacillus, Blautia,* and *Oscillospira* in the stabilization period. There is no evidence that *Shigella* can ferment propionate, but it can use propionate as a carbon or energy source, which is significantly negatively related to propionate (Tao et al., 2022). In addition, among the highly abundant bacteria during the colonization period, some were closely related to propionate fermentation, such as *Clostridium, Butyricicoccus* and *Peptostreptococcus*. *Shigella* and propionate-fermenting bacteria may have some interactions in the intestine, such as competing for nutrients and affecting the intestinal pH and microbial balance. The interactions between *Shigella* and *Clostridium* or between *Butyricicoccus* and *Peptostreptococcus* may influence the efficiency of propionate fermentation, but the specific mechanism involved needs further investigation.

5. Conclusion

A dynamic distribution of the microbiota and metabolic function in the rectums of neonatal calves during the first 10 weeks of age was observed in the present study. The colonization process of the bacterial genera could be divided into 2 periods and 5 stages: stage 1 (d 1), stage 2 (d 3), stage 3 (d 7-14), stage 4 (d 21-42), and stage 5 (d 49-70). The colonization period included stages 1 and 2, and the stable period included stages 3 to 5. The highly abundant genera and the fermentation pattern differed between the colonization period and stable period, and the stable period had more diverse and complex metabolic functions than did the colonization period. During the colonization period, VFA production and degradation occurred mainly via the propionate fermentation pattern dominated by *Shigella*. During the stable period, VFA production and degradation were dominated by *Lactobacillus, Blautia,* and *Oscillospira,* which are involved in many metabolic pathways and are mainly based on the lactic acid fermentation pattern. The changes in fermentation pattern and metabolic function may be related to the colonization of these genera at stage 3 (*Lactobacillus, Dorea, Collinsella,* and *[Ruminococcus]*) in the gut of young calves. As the digestive tracts of calves gradually adapt to starter feeding, the intestinal microbiota undergoes a transition period. During this period, the abundance of *Lactobacillus* increased, which gradually decreased the abundance of harmful bacteria (such as Proteobacteria and *Shigella*). Therefore, it is important to provide strict management and appropriate preventive measures to calves during their early life, and nutritional interventions that promote *Lactobacillus* colonization may be the key strategy to prevent and control the occurrence of diarrhea or other gastrointestinal disorders.

Credit Author Statement

Qi Huang: Data curation, Investigation, Methodology, Writing - original draft. **Fengtao Ma**, **Yuhang Jin** and **Duo Gao**: Investigation, Methodology. **Meinan Chang**: Writing - review & editing. **Peng Sun**: Supervision, Writing - review & editing, Funding acquisition, Project administration, Conceptualization.

Date availability statements

The 16S rRNA sequencing data for all the samples were deposited into the NCBI Sequence Read Archive (SRA) under accession number SRP320638 (https://www.ncbi.nlm.nih.gov/sra/?term=SRP320638).

Declaration of competing interest

We declare that we have no financial or personal relationships with other people or organizations that can inappropriately influence our work, and there is no professional or other personal interest of any nature or kind in any product, service or company that could be construed as influencing the content of this paper.

Acknowledgement

This study was supported by the National Key Research and Development Program of China (2022YFD1300505; 2022YFD1301101), the earmarked fund for the China Agriculture Research System (CARS-37), and the Agricultural Science and Technology Innovation Program (cxgc-ias-07).

Appendix A. Supplementary data

Supplementary data to this article can be found online at https://doi.org/10.1016/j.aninu.2024.06.007.

References

AOAC International. Official methods of analysis. 18th ed. Washington, VA: AOAC International; 2000.
AOAC International. Official methods of analysis. 18th ed. Washington, MD: AOAC International; 2003.
AOAC International. Official methods of analysis. 18th ed. Washington, DC: AOAC International; 2005.
Arrieta MC, Stiemsma LT, Amenyogbe N, Brown EM, Finlay B. The intestinal microbiome in early life: health and disease. Front Immunol 2014;5:427.
Bi Y, Tu Y, Zhang N, Wang S, Zhang F, Suen G, Shao D, Li S, Diao Q. Multiomics analysis reveals the presence of a microbiome in the gut of fetal lambs. Gut 2021;70:853–64.
Bokulich NA, Kaehler BD, Rideout JR, Dillon M, Bolyen E, Knight R, Huttley GA, Gregory Caporaso J. Optimizing taxonomic classification of marker-gene amplicon sequences with qiime 2's q2-feature-classifier plugin. Microbiome 2018;6:90.
Bolyen E, Rideout JR, Dillon M, Bokulich N, Abnet C, Al-Ghalith G, Alexander H, Alm E, Arumugam M, Asnicar F, Bai Y, Bisanz J, Bittinger K, Brejnrod A, Brislawn C, Brown CT, Callahan B, Caraballo Rodríguez A, Chase J, Caporaso J. Qiime 2: reproducible, interactive, scalable, and extensible microbiome data science. 2018.
Breiman L. Random forests. Mach Learn 2001;45:5–32.

Callahan BJ, Mcmurdie PJ, Rosen MJ, Han AW, Johnson AJ, Holmes SP. Dada2: high-resolution sample inference from illumina amplicon data. Nat Methods 2016;13:581–3.
Cani PD, Amar J, Iglesias MA, Poggi M, Knauf C, Bastelica D, Neyrinck AM, Fava F, Tuohy KM, Chabo C, Waget A, Delmée E, Cousin B, Sulpice T, Chamontin B, Ferrières J, Tanti JF, Gibson GR, Casteilla L, Delzenne NM, Alessi MC, Burcelin R. Metabolic endotoxemia initiates obesity and insulin resistance. Diabetes 2007;56:1761–72.
Cascone T, Weissferdt A, Godoy MCB, William Jr WN, Leung CH, Lin HY, Basu S, Yadav SS, Pataer A, Mitchell KG, Khan MaW, Shi Y, Haymaker C, Solis LM, Parra ER, Kadara H, Wistuba Ii, Sharma P, Allison JP, Ajami NJ, Wargo JA, Jenq RR, Gibbons DL, Lee JJ, Swisher SG, Vaporciyan AA, Heymach JV, Sepesi B. Nodal immune flare mimics nodal disease progression following neoadjuvant immune checkpoint inhibitors in non-small cell lung cancer. Nat Commun 2021;12:5045.
Caspi R, Billington R, Ferrer L, Foerster H, Fulcher CA, Keseler IM, Kothari A, Krummenacker M, Latendresse M, Mueller LA, Ong Q, Paley S, Subhraveti P, Weaver DS, Karp PD. The metacyc database of metabolic pathways and enzymes and the biocyc collection of pathway/genome databases. Nucleic Acids Res 2016;44:D471–80.
Chang MN, Wei JY, Hao LY, Ma FT, Li HY, Zhao SG, Sun P. Effects of different types of zinc supplement on the growth, incidence of diarrhea, immune function, and rectal microbiota of newborn dairy calves. J Dairy Sci 2020;103:6100–13.
Chang M, Wang F, Ma F, Jin Y, Sun P. Supplementation with galacto-oligosaccharides in early life persistently facilitates the microbial colonization of the rumen and promotes growth of preweaning holstein dairy calves. Anim Nutr 2022;10:223–33.
Cheirsilp B, Shimizu H, Shioya S. Enhanced kefiran production by mixed culture of lactobacillus kefiranofaciens and saccharomyces cerevisiae. J Biotechnol 2003;100:43–53.
Chen H, Liu Y, Huang K, Yang B, Zhang Y, Yu Z, Wang J. Fecal microbiota dynamics and its relationship to diarrhea and health in dairy calves. J Anim Sci Biotechnol 2022;13:132.
Choudhury R, Middelkoop A, Bolhuis JE, Kleerebezem M. Legitimate and reliable determination of the age-related intestinal microbiome in young piglets; rectal swabs and fecal samples provide comparable insights. Front Microbiol 2019;10:1886.
Dill-Mcfarland KA, Breaker JD, Suen G. Microbial succession in the gastrointestinal tract of dairy cows from 2 weeks to first lactation. Sci Rep 2017;7:40864.
Douglas GM, Maffei VJ, Zaneveld JR, Yurgel SN, Brown JR, Taylor CM, Huttenhower C, Langille MGI. Picrust2 for prediction of metagenome functions. Nat Biotechnol 2020;38:685–8.
Ernst J, Bar-Joseph Z. Stem: a tool for the analysis of short time series gene expression data. BMC Bioinf 2006;7:191.
Fan P, Nelson CD, Driver JD, Elzo MA, Peñagaricano F, Jeong KC. Host genetics exerts lifelong effects upon hindgut microbiota and its association with bovine growth and immunity. ISME J 2021;15:2306–21.
Gonzalez A, Krieg R, Massey HD, Carl D, Ghosh S, Gehr TWB, Ghosh SS. Sodium butyrate ameliorates insulin resistance and renal failure in ckd rats by modulating intestinal permeability and mucin expression. Nephrol Dial Transplant 2019;34:783–94.
Jami E, Israel A, Kotser A, Mizrahi I. Exploring the bovine rumen bacterial community from birth to adulthood. ISME J 2013;7:1069–79.
Jordan HV. Cariogenic flora: establishment, localization, and transmission. J Dent Res 1976;55(Spec No):C10–4.
Jost T, Lacroix C, Braegger CP, Chassard C. New insights in gut microbiota establishment in healthy breast fed neonates. PLoS One 2012;7:e44595.
Katoh K, Misawa K, Kuma K, Miyata T. Mafft: a novel method for rapid multiple sequence alignment based on fast fourier transform. Nucleic Acids Res 2002;30:3059–66.
Kechin A, Boyarskikh U, Kel A, Filipenko M. Cutprimers: a new tool for accurate cutting of primers from reads of targeted next generation sequencing. J Comput Biol 2017;24:1138–43.
Kim HS, Whon TW, Sung H, Jeong YS, Jung ES, Shin NR, Hyun DW, Kim PS, Lee JY, Lee CH, Bae JW. Longitudinal evaluation of fecal microbiota transplantation for ameliorating calf diarrhea and improving growth performance. Nat Commun 2021;12:161.
Klein-Jöbstl D, Quijada NM, Dzieciol M, Feldbacher B, Wagner M, Drillich M, Schmitz-Esser S, Mann E. Microbiota of newborn calves and their mothers reveals possible transfer routes for newborn calves' gastrointestinal microbiota. PLoS One 2019;14:e0220554.
Li B, Zhang K, Li C, Wang X, Chen Y, Yang Y. Characterization and comparison of microbiota in the gastrointestinal tracts of the goat (capra hircus) during preweaning development. Front Microbiol 2019;10:2125.
Liu X, Zhao K, Yang X, Zhao Y. Gut microbiota and metabolome response of decaisnea insignis seed oil on metabolism disorder induced by excess alcohol consumption. J Agric Food Chem 2019;67:10667–77.
Liu Z, Luo G, Du R, Sun W, Li J, Lan H, Chen P, Yuan X, Cao D, Li Y, Liu C, Liang S, Jin X, Yang R, Bi Y, Han Y, Cao P, Zhao W, Ling S, Li Y. Effects of spaceflight on the composition and function of the human gut microbiota. Gut Microb 2020;11:807–19.
Lozupone C, Knight R. Unifrac: a new phylogenetic method for comparing microbial communities. Appl Environ Microbiol 2005;71:8228–35.
Lozupone CA, Hamady M, Kelley ST, Knight R. Quantitative and qualitative beta diversity measures lead to different insights into factors that structure microbial communities. Appl Environ Microbiol 2007;73:1576–85.
Luo Z, Ma L, Zhou T, Huang Y, Zhang L, Du Z, Yong K, Yao X, Shen L, Yu S, Shi X, Cao S. Beta-glucan alters gut microbiota and plasma metabolites in pre-weaning dairy calves. Metabolites 2022;12.
Ma T, Villot C, Renaud D, Skidmore A, Chevaux E, Steele M, Guan LL. Linking perturbations to temporal changes in diversity, stability, and compositions of neonatal calf gut microbiota: prediction of diarrhea. ISME J 2020;14:2223–35.
Malmuthuge N, Liang G, Guan LL. Regulation of rumen development in neonatal ruminants through microbial metagenomes and host transcriptomes. Genome Biol 2019;20:172.
Marteyn B, West NP, Browning DF, Cole JA, Shaw JG, Palm F, Mounier J, Prévost MC, Sansonetti P, Tang CM. Modulation of shigella virulence in response to available oxygen in vivo. Nature 2010;465:355–8.
Mcdonald D, Price MN, Goodrich J, Nawrocki EP, Desantis TZ, Probst A, Andersen GL, Knight R, Hugenholtz P. An improved greengenes taxonomy with explicit ranks for ecological and evolutionary analyses of bacteria and archaea. ISME J 2012;6:610–8.
Mirpuri J, Raetz M, Sturge CR, Wilhelm CL, Benson A, Savani RC, Hooper LV, Yarovinsky F. Proteobacteria-specific iga regulates maturation of the intestinal microbiota. Gut Microb 2014;5:28–39.
Nuli R, Cai J, Kadeer A, Zhang Y, Mohemaiti P. Integrative analysis toward different glucose tolerance-related gut microbiota and diet. Front Endocrinol 2019;10:295.
Pempek JA, Watkins LR, Bruner CE, Habing GG. A multisite, randomized field trial to evaluate the influence of lactoferrin on the morbidity and mortality of dairy calves with diarrhea. J Dairy Sci 2019;102:9259–67.
Price MN, Dehal PS, Arkin AP. Fasttree 2–approximately maximum-likelihood trees for large alignments. PLoS One 2010;5:e9490.
Quijada NM, Bodas R, Lorenzo JM, Schmitz-Esser S, Rodríguez-Lázaro D, Hernández M. Dietary supplementation with sugar beet fructooligosaccharides and garlic residues promotes growth of beneficial bacteria and increases weight gain in neonatal lambs. Biomolecules 2020;10.
Ramette A. Multivariate analyses in microbial ecology. FEMS Microbiol Ecol 2007;62:142–60.
Rey M, Enjalbert F, Combes S, Cauquil L, Bouchez O, Monteils V. Establishment of ruminal bacterial community in dairy calves from birth to weaning is sequential. J Appl Microbiol 2014;116:245–57.
Rizzatti G, Lopetuso LR, Gibiino G, Binda C, Gasbarrini A. Proteobacteria: a common factor in human diseases. BioMed Res Int 2017;2017:9351507.
Ronan V, Yeasin R, Claud EC. Childhood development and the microbiome-the intestinal microbiota in maintenance of health and development of disease during childhood development. Gastroenterology 2021;160:495–506.
Schwaiger K, Storch J, Bauer C, Bauer J. Abundance of selected bacterial groups in healthy calves and calves developing diarrhea during the first week of life: are there differences before the manifestation of clinical symptoms? Front Microbiol 2022;13:958080.
Segata N, Izard J, Waldron L, Gevers D, Miropolsky L, Garrett WS, Huttenhower C. Metagenomic biomarker discovery and explanation. Genome Biol 2011;12:R60.
Shin NR, Whon TW, Bae JW. Proteobacteria: microbial signature of dysbiosis in gut microbiota. Trends Biotechnol 2015;33:496–503.
Smith HW. The development of the flora of the alimentary tract in young animals. J Pathol Bacteriol 1965;90:495–513.
Sokol H, Leducq V, Aschard H, Pham HP, Jegou S, Landman C, Cohen D, Liguori G, Bourrier A, Nion-Larmurier I, Cosnes J, Seksik P, Langella P, Skurnik D, Richard ML, Beaugerie L. Fungal microbiota dysbiosis in ibd. Gut 2017;66:1039–48.
Standardization Administration of the People's Republic of China. GB/T 3157-2023. Chinese Holstein. 2023. Beijing.
Stevenson DM, Weimer PJ. Dominance of prevotella and low abundance of classical ruminal bacterial species in the bovine rumen revealed by relative quantification real-time pcr. Appl Microbiol Biotechnol 2007;75:165–74.
Tao W, Liu W, Wang M, Zhou W, Xing J, Xu J, Pi X, Wang X, Lu S, Yang Y. Dendrobium officinale polysaccharides better regulate the microbiota of women than men. Foods 2022;11.
Tian X, Yu Z, Feng P, Ye Z, Li R, Liu J, Hu J, Kakade A, Liu P, Li X. Lactobacillus plantarum tw1-1 alleviates diethylhexylphthalate-induced testicular damage in mice by modulating gut microbiota and decreasing inflammation. Front Cell Infect Microbiol 2019;9:221.
USDA. Average daily gain of pre-weaned holstein heifer calves. NAHMS dairy 2014 study calf component 2021:2–4. https://www.aphis.usda.gov/sites/default/files/adg-preweaned-holstein-heifer.pdf.
Valdes AM, Walter J, Segal E, Spector TD. Role of the gut microbiota in nutrition and health. BMJ 2018;361:k2179.
Van Soest PJ, Robertson JB, Lewis BA. Methods for dietary fiber, neutral detergent fiber, and nonstarch polysaccharides in relation to animal nutrition. J Dairy Sci 1991;74:3583–97.
Vassallo G, Mirijello A, Ferrulli A, Antonelli M, Landolfi R, Gasbarrini A, Addolorato G. Review article: alcohol and gut microbiota - the possible role of gut microbiota modulation in the treatment of alcoholic liver disease. Aliment Pharmacol Ther 2015;41:917–27.
Vergara-Irigaray M, Fookes MC, Thomson NR, Tang CM. Rna-seq analysis of the influence of anaerobiosis and fnr on shigella flexneri. BMC Genom 2014;15:438.

Wang J, Hu R, Wang Z, Guo Y, Wang S, Zou H, Peng Q, Jiang Y. Establishment of immortalized yak ruminal epithelial cell lines by lentivirus-mediated sv40t and htert gene transduction. Oxid Med Cell Longev 2022;2022:8128028.
Warton DI, Wright ST, Wang YaJMIE, Evolution. Distance-based multivariate analyses confound location and dispersion effects. Method Ecol Evol 2012;3.
Xiao L, Wang J, Zheng J, Li X, Zhao F. Deterministic transition of enterotypes shapes the infant gut microbiome at an early age. Genome Biol 2021;22:243.
Xu R, Ding Z, Zhao P, Tang L, Tang X, Xiao S. The effects of early post-operative soluble dietary fiber enteral nutrition for colon cancer. Nutrients 2016;8.
Xue MY, Sun HZ, Wu XH, Liu JX, Guan LL. Multi-omics reveals that the rumen microbiome and its metabolome together with the host metabolome contribute to individualized dairy cow performance. Microbiome 2020;8:64.
Yeoman CJ, Ishaq SL, Bichi E, Olivo SK, Lowe J, Aldridge BM. Biogeographical differences in the influence of maternal microbial sources on the early successional development of the bovine neonatal gastrointestinal tract. Sci Rep 2018;8:3197.
Yu X, Wo Y, Ma F, Shan Q, Wei J, Sun P. Zinc methionine improves the lipid metabolism that is associated with the alteration of intestine mucosal proteomes and microbiota of newborn holstein dairy calves. Animal Research and One Health 2024;2(1):71–85.